Please cite this article in press as: Hoogerheide et al., Real-Time Nanopore-Based Recognition of Protein Translocation Success, Biophysical Journal (2018), https://doi.org/10.1016/j.bpj.2017.12.019

Biophysical *Journal*
Biophysical Letter

Biophysical Society

Real-Time Nanopore-Based Recognition of Protein Translocation Success

David P. Hoogerheide,[1,*] Philip A. Gurnev,[2] Tatiana K. Rostovtseva,[2] and Sergey M. Bezrukov[2,*]
[1]Center for Neutron Research, National Institute of Standards and Technology, Gaithersburg, Maryland and [2]Section on Molecular Transport, Eunice Kennedy Shriver National Institute of Child Health and Human Development, National Institutes of Health, Bethesda, Maryland

ABSTRACT A growing number of new technologies are supported by a single- or multi-nanopore architecture for capture, sensing, and delivery of polymeric biomolecules. Nanopore-based single-molecule DNA sequencing is the premier example. This method relies on the uniform linear charge density of DNA, so that each DNA strand is overwhelmingly likely to pass through the nanopore and across the separating membrane. For disordered peptides, folded proteins, or block copolymers with heterogeneous charge densities, by contrast, translocation is not assured, and additional strategies to monitor the progress of the polymer molecule through a nanopore are required. Here, we demonstrate a single-molecule method for direct, model-free, real-time monitoring of the translocation of a disordered, heterogeneously charged polypeptide through a nanopore. The crucial elements are two "selectivity tags"—regions of different but uniform charge density—at the ends of the polypeptide. These affect the selectivity of the nanopore differently and enable discrimination between polypeptide translocation and retraction. Our results demonstrate exquisite sensitivity of polypeptide translocation to applied transmembrane potential and prove the principle that nanopore selectivity reports on biopolymer substructure. We anticipate that the selectivity tag technique will be broadly applicable to nanopore-based protein detection, analysis, and separation technologies, and to the elucidation of protein translocation processes in normal cellular function and in disease.

A nanopore is a single nanometer-scale hole in a thin membrane that separates two electrolyte-filled reservoirs. Nanopores can be created using both solid-state (1) and biological (2) materials and are sensitive single-molecule probes and manipulators of charged biopolymers (3–8). The electric field resulting from a voltage bias applied across the membrane creates an ionic current that can be monitored in real time. Individual charged, polymeric biomolecules are captured in the nanopore and eventually escape, causing a transient disruption in the ionic current. The time-dependent characteristics of each disruption, or "event," contain information about the motion and structure of the captured polymer.

The overwhelming majority of nanopore studies have used single-stranded or double-stranded DNA as an analyte, mainly due to the technological importance of DNA sequencing (9–11). The ultimate success of DNA-sequencing technologies, in which engineered nanopores (12) are augmented with molecular machinery to control the motion of the DNA strand (13,14), is due in part to the homogeneous, sequence-independent charge density of the DNA phosphate backbone (or the homogeneous charge density of cleavage products in sequencing by synthesis strategies (7)). One important consequence of this fact is that although thermal forces may contribute to rapid backward fluctuations of the polymer (15), the average electrical force is sequence-independent and unidirectional, and at high enough voltages, each strand passes through the nanopore, or "translocates," with unity probability, rather than retracting to the side of the entry. This has been demonstrated experimentally using polymerase chain reaction (2) and a variety of nanopore-based single-molecule trapping techniques (16–18).

For the many other synthetic and biological polymers, such as proteins (19,20), in which monomers can be anionic, cationic, or uncharged, the electrical force is sequence-dependent and, in principle, bidirectional. Thus, even a question as fundamental as whether a given biopolymer ever translocates through a nanopore becomes difficult to answer, particularly in the absence of amplification methods such as those used for DNA. Previous experimental studies of protein translocation through nanopores employed processive enzymes (21), overrode the native charge density with surfactant (22), or used homogenously charged peptides (23) to provide unidirectional motion.

Submitted September 29, 2017, and accepted for publication December 15, 2017.

*Correspondence: david.hoogerheide@nist.gov or bezrukos@mail.nih.gov
Editor: Chris Chipot.
https://doi.org/10.1016/j.bpj.2017.12.019

Please cite this article in press as: Hoogerheide et al., Real-Time Nanopore-Based Recognition of Protein Translocation Success, Biophysical Journal (2018), https://doi.org/10.1016/j.bpj.2017.12.019

Here, we study translocation of a heterogeneously charged polypeptide using model-free detection of the effect of the polymer charge on the electrical environment inside the nanopore to monitor the translocation process of single polypeptides in real time. This is accomplished using "selectivity tags"—regions of different but uniform charge density at the ends of a polypeptide that produce different selectivity of the nanopore to cations and anions, and hence ionic current levels, in a voltage-biased nanopore under a salt concentration gradient. We use the natural, disordered "diblock copolymer"-like 140-amino-acid polypeptide α-synuclein (α-syn), which comprises two such tags, a highly negatively charged C-terminal region (CT; 43 amino acids, total charge $-15e$) and a largely neutral N-terminal region (NT; 97 amino acids, total charge $+3e$). The CT is responsible for capture of α-syn into the voltage-biased nanopore, whereas the NT is responsible for binding to lipid membrane surfaces and ensures that the α-syn molecule remains in the pore long enough for its dynamics to be extensively studied (24). The boundary between the CT and NT fluctuates across the membrane, exposing the pore to the differing charge densities of the CT and NT and modulating the selectivity of the pore, which is monitored in real time using an electrolyte concentration gradient. The selectivity at the end of each α-syn capture event depends on whether the last residues in the pore were charged (a "retraction event," in which the CT withdraws from the nanopore) or uncharged (a "translocation event," in which the NT is observed last). The voltage-dependent translocation probability derived in this way corresponds well to, but does not require, the drift-diffusion models previously developed for the α-syn/nanopore and DNA/nanopore systems (20,25).

The experimental setup is shown in Fig. 1 *a*. The nanopore is a single mitochondrial passive ATP/ADP-transport voltage-dependent anion channel (VDAC) reconstituted into a diphytanoylphosphatidylcholine lipid bilayer membrane separating 1.0 M (*trans*) and 0.2 M (*cis*) aqueous solutions of potassium chloride (M = mol/L). When α-syn is added to the *trans* side of the membrane (see the Materials and Methods), large current blockages are observed. At concentrations sufficiently small to suppress simultaneous interaction of multiple α-syn molecules with the VDAC, fluctuations between two well-defined levels, or substates, within these large current blockages are further detected (Fig. 1, *b* and *c*). A current-voltage plot (Fig. 1 *b*) of the substates (averaged over the thousands of blockages observed over multiple voltages in a single experiment) shows that the selectivity of the pore, as reported by its reversal potential (*vertical arrows*), differs by 20 mV between the two substates and reverses from anionic to cationic. In previous work this splitting was hypothesized, based on electrostatic considerations, to correspond to the presence of the charged or uncharged regions (within the 5- to 10-residue resolution of VDAC) of the α-syn molecule in the pore (20). Here, we directly observe the relationship between the states by analyzing the fine structure of each event.

For all blockages, the event begins in the lower-conducting substate, allowing us to identify this state as the one corresponding to the presence of the CT in the pore, that is, to the capture of the C-terminal region of α-syn by the VDAC nanopore (Fig. 1 *d*). We label this substate S_C and, by elimination, the higher-conducting substate S_N. This identification allows us to classify each event in a model-free (i.e., independent of prior knowledge of the nanopore electrostatic properties) way as a retraction or translocation event based on the substate observed at the end of the event. Fig. 1 *e* shows a retraction event, in which the final substate (S_C) is the same as the initial one and corresponds to the withdrawal of the CT from the pore. Fig. 1 *f*, by contrast, shows a translocation event, in which the final substate (S_N) is different from the initial one and corresponds to the passage of the NT—and hence the whole α-syn molecule—through the pore.

Importantly, the fraction of translocation events, i.e., the translocation probability, is determined from this characterization of events on the single-molecule level. The observed translocation probability depends strongly on voltage and is shown in Fig. 2 *a* as red circles. The blue diamonds depict the result of applying a simple correction that takes into account the limited temporal resolution of the instrumentation, as described in the Supporting Material. Fig. 2 *b* gives the average event duration $\langle\tau\rangle$ as a function of voltage. The solid lines are fits to a drift-diffusion model for this system described elsewhere (20) and modified with an additional constant-force term corresponding to hydrodynamic drag from an osmotically driven flow of water from the low-salt to the high-salt side of the channel (see the Supporting Material). The model is optimized to the event duration distributions, but not to the translocation probability data; the solid line in Fig. 2 *a* is the prediction of the translocation probability from the model with no additional optimization. The agreement is good to within 1 mV, particularly for the resolution-corrected data.

The average properties of retraction and translocation events are explored separately in Fig. 3. The vertical axis is the average CT occupancy as a function of time from the beginning (Fig. 3 *a*) or end (Fig. 3 *b*) of the event. Fig. 3 *a* shows that the probabilistic average event shape at the beginning of the event does not depend on its identification as a retraction or translocation. The initial capture process is too fast to be reliably observed given the noise level and temporal resolution of the system and instrumentation, resulting in an average CT occupancy less than unity at the beginning of events. The capture process only becomes shorter at higher voltages, resulting in further deviations from unity. Fig. 3 *b* shows that the dynamics of the final states are significantly different: the final translocation process takes almost 10 times longer than the retraction process.

Please cite this article in press as: Hoogerheide et al., Real-Time Nanopore-Based Recognition of Protein Translocation Success, Biophysical Journal (2018), https://doi.org/10.1016/j.bpj.2017.12.019

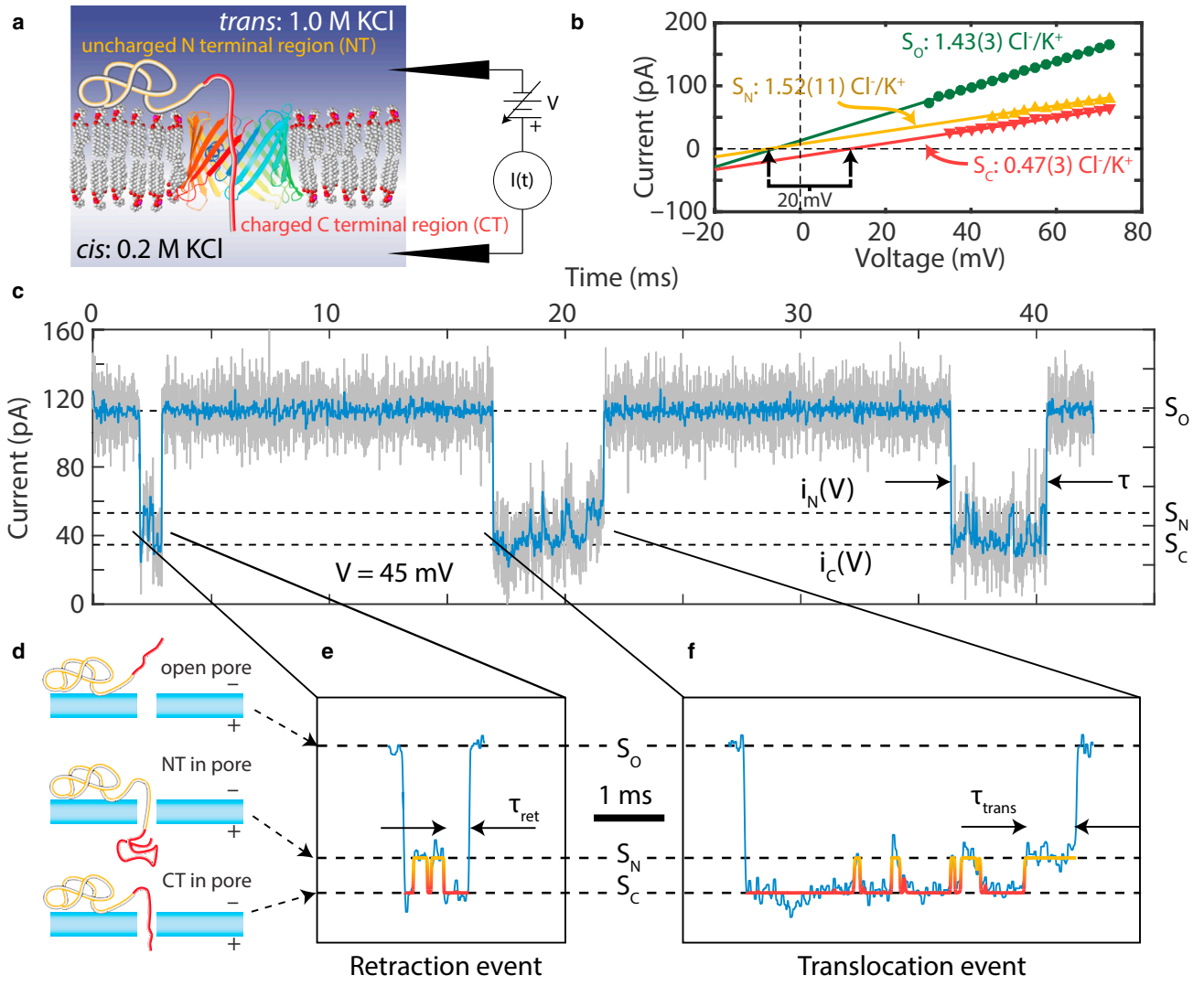

FIGURE 1 Salt-concentration-gradient-enhanced observation of α-syn dynamics in a VDAC nanopore. (*a*) Experimental setup (not to scale). The "diblock-copolymer"-like structure of α-syn is represented in color and consists of two "selectivity tags" of differing charge density (*light yellow* and *dark red*) that differently modulate the electrical properties of the VDAC nanopore under a salt concentration gradient. (*b*) Current-voltage curves of the open pore high-conducting (*dark green circles*) and the two low-conducting substates when α-syn is inside the pore (*yellow triangles* and *red inverted triangles*). Selectivities were calculated from the reversal potentials (*vertical arrows*); 68% confidence intervals are smaller than the size of the data points. (*c*) Sample current record. As-recorded data are shown in light gray and software-filtered data in dark blue. The total event duration, τ, was defined as shown. (*d*) Identification of the substates by noting that the capture of the CT in the nanopore corresponds to the lower-conducting substate. (*e* and *f*) Details of a retraction (*e*) and a translocation (*f*) event. The smooth overlay curve depicts $P_C(t)$ using the scaled representation $i_C(V)+(1-P_C(t))(i_N(V)-i_C(V))$ and a color scale between $P_C(t)=0$ (*light yellow*) and 1 (*dark red*). To see this figure in color, go online.

The selectivity-tag method is quite general. With sufficient time resolution and current sensitivity, the technique can be performed by simply comparing the selectivity of the pore (manifested as distinctly different current levels under the salt-gradient conditions) during the capture and release processes of individual polypeptides, with no requirement of prior knowledge of the molecule's sequence and no need to average over large populations of molecules. It can thus be used to identify minor components of complex mixtures. Although routine use would benefit from a well-characterized pore, the method does not have specific requirements for the nanopore type. Selectivity tags can be incorporated into folded proteins and polypeptides using standard biotechnology techniques, or into block copolymers using standard synthesis methods. In these experiments, selectivity tags were used to determine which events corresponded to α-syn translocations. In principle, however, a selectivity tag can be integrated into the interior of a molecule, to track its progress through the pore; at both ends of a molecule, to signal that one or the other end is about to leave

Please cite this article in press as: Hoogerheide et al., Real-Time Nanopore-Based Recognition of Protein Translocation Success, Biophysical Journal (2018), https://doi.org/10.1016/j.bpj.2017.12.019

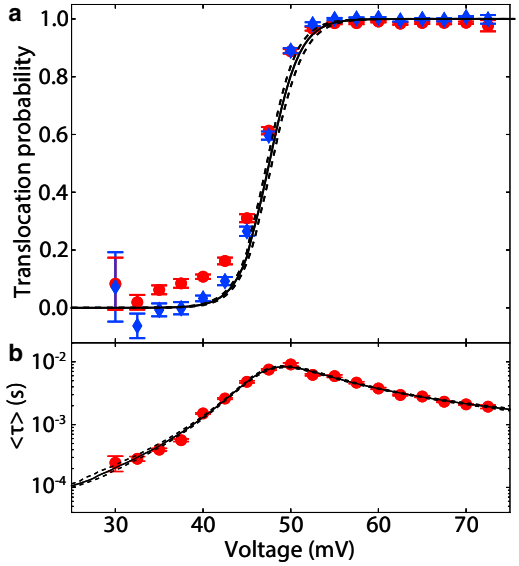

FIGURE 2 Direct experimental observation of translocation probability. (*a*) Fraction of events in which the uncharged selectivity tag was observed at the end of the event. Red circles represent the observed translocation probability; blue diamonds are corrected for the limited temporal resolution of the instrumentation. Error bars represent 68% confidence intervals. The solid line is the prediction of the drift-diffusion stochastic model for this system, whereas the dashed lines show 95% confidence intervals for this prediction. The model was optimized to the composite histograms of total event duration including both translocation and retraction events, but not to the experimentally measured translocation probability curve. (*b*) Average event durations with the optimized model. The average event duration is maximal at a transmembrane voltage of 50 mV, which corresponds to a pulling force on the CT of ≈7.4 pN. To see this figure in color, go online.

the nanopore, with the possibility of employing active feedback to retain or discard the molecule; or at various points along a molecule, to study fluctuations and translocation dynamics. For these applications, careful validation of labeled protein function would be required. The sensitivity of the translocation probability to voltage also suggests that the use of selectivity tags may be a powerful separation method for complex mixtures of biomolecules that yield otherwise indistinguishable or overlapping resistive pulse signals. Selectivity tags provide an additional recognition dimension for direct protein sequencing or for techniques like sequencing by synthesis (7), which require discrimination of cleavage products. Finally, this work opens an avenue to solving long-standing, medically relevant questions regarding protein translocation, such as bacterial toxicity mechanisms (26,27) and the operation of cellular protein transport machinery (28).

Materials and methods

Protein purification protocols are described in the Supporting Material. Single VDAC channel recordings were obtained as described previously (24). Lipid bilayers were formed from diphytanoylphosphatidylcholine. The side of the lipid bilayer to which VDAC was added during the reconstitution is the *cis* side; the opposite side is referred to as the *trans* side (Fig. 1 *a*). Voltage polarities are defined as positive when the *cis* side has the higher potential. To create the salt concentration gradient, the *cis* side was filled with a 0.2 M KCl solution (M = mol/L) and the *trans* side with a 1.0 M KCl solution, both buffered with 5 mM HEPES at pH 7.4. Junction potentials with the Ag/AgCl electrodes were minimized by connecting the electrodes with 2 M KCl/2% agarose bridges. Recombinant α-syn was added to the *trans* side at 5–10 nM concentrations. The low α-syn concentration was chosen to minimize the incidence of simultaneous pore blockage by multiple molecules. Current recordings at each voltage were collected by an Axopatch 200B amplifier (Molecular Devices, Sunnydale, CA) with a 4 μs sampling interval, hardware filtered by a 30 kHz inline eight-pole Bessel filter (9002; Frequency Devices, Ottawa, IL), and directly saved into computer memory with Clampex 10 software (Molecular Devices).

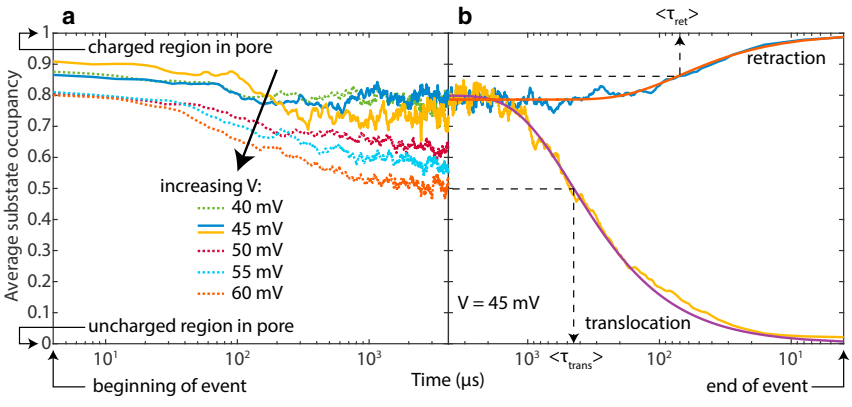

FIGURE 3 Average properties of retraction and translocation events. The substate occupancy is defined to be 0 when the NT is in the pore and 1 when the CT is in the pore. (*a*) Average substate occupancy as a function of time from the beginning of the event. Solid blue and yellow curves were averaged over retraction and translocation events, respectively, observed at a 45 mV transmembrane voltage, showing that both types of events begin with the charged region in the pore. Dotted lines are averages over all events at other voltages. Deviations from unity are caused by limited temporal resolution of the measurement, and they increase as the capture process shortens at higher voltages. (*b*) Average substate occupancy as a function of time from the end of the event, averaged over all retraction (*top*) and translocation (*bottom*) events. Average occupancy is fit by an exponential function that yields the characteristic timescales of the retraction $\langle\tau_{ret}\rangle$ and translocation $\langle\tau_{trans}\rangle$ processes. To see this figure in color, go online.

Please cite this article in press as: Hoogerheide et al., Real-Time Nanopore-Based Recognition of Protein Translocation Success, Biophysical Journal (2018), https://doi.org/10.1016/j.bpj.2017.12.019

All experiments were performed at room temperature (22 ± 2°C). The experiment was replicated four times. Analysis and modeling procedures are detailed in the Supporting Material.

SUPPORTING MATERIAL

Supporting Materials and Methods, two figures, and one table are available at http://www.biophysj.org/biophysj/supplemental/S0006-3495(17)35099-3.

AUTHOR CONTRIBUTIONS

P.G. performed research, and D.H. analyzed and modeled the data. All authors designed the research and wrote the manuscript.

ACKNOWLEDGMENTS

The authors are grateful to Dr. Jennifer Lee of National Heart, Lung, and Blood Institute, National Institutes of Health for the generous gift of recombinant α-synuclein protein. Certain commercial materials, equipment, and instruments are identified in this work to describe the experimental procedure as completely as possible. In no case does such an identification imply a recommendation or endorsement by the National Institute of Standards and Technology, nor does it imply that the materials, equipment, or instrument identified are necessarily the best available for the purpose.

This work used the Extreme Science and Engineering Discovery Environment (XSEDE), which is supported by National Science Foundation grant number ACI-1053575. Specifically, it used the Bridges system, which is supported by National Science Foundation award number ACI-1445606, at the Pittsburgh Supercomputing Center (PSC). P.A.G., T.K.R., and S.M.B. were supported by the Intramural Research Program of the Eunice Kennedy Shriver National Institute of Child Health and Human Development, National Institutes of Health.

REFERENCES

1. Li, J., D. Stein, …, J. A. Golovchenko. 2001. Ion-beam sculpting at nanometre length scales. *Nature.* 412:166–169.
2. Kasianowicz, J. J., E. Brandin, …, D. W. Deamer. 1996. Characterization of individual polynucleotide molecules using a membrane channel. *Proc. Natl. Acad. Sci. USA.* 93:13770–13773.
3. Laszlo, A. H., I. M. Derrington, and J. H. Gundlach. 2016. MspA nanopore as a single-molecule tool: from sequencing to SPRNT. *Methods.* 105:75–89.
4. Hernández-Ainsa, S., and U. F. Keyser. 2014. DNA origami nanopores: developments, challenges and perspectives. *Nanoscale.* 6:14121–14132.
5. Larkin, J., M. Foquet, …, M. Wanunu. 2014. Reversible positioning of single molecules inside zero-mode waveguides. *Nano Lett.* 14:6023–6029.
6. Yusko, E. C., B. R. Bruhn, …, M. Mayer. 2017. Real-time shape approximation and fingerprinting of single proteins using a nanopore. *Nat. Nanotechnol.* 12:360–367.
7. Kumar, S., C. Tao, …, J. Ju. 2012. PEG-labeled nucleotides and nanopore detection for single molecule DNA sequencing by synthesis. *Sci. Rep.* 2:684.
8. Plesa, C., S. W. Kowalczyk, …, C. Dekker. 2013. Fast translocation of proteins through solid state nanopores. *Nano Lett.* 13:658–663.
9. Branton, D., D. W. Deamer, …, J. A. Schloss. 2008. The potential and challenges of nanopore sequencing. *Nat. Biotechnol.* 26:1146–1153.
10. Bayley, H. 2015. Nanopore sequencing: from imagination to reality. *Clin. Chem.* 61:25–31.
11. Deamer, D., M. Akeson, and D. Branton. 2016. Three decades of nanopore sequencing. *Nat. Biotechnol.* 34:518–524.
12. Astier, Y., O. Braha, and H. Bayley. 2006. Toward single molecule DNA sequencing: direct identification of ribonucleoside and deoxyribonucleoside 5′-monophosphates by using an engineered protein nanopore equipped with a molecular adapter. *J. Am. Chem. Soc.* 128:1705–1710.
13. Chu, J., M. González-López, …, M. R. Ghadiri. 2010. Real-time monitoring of DNA polymerase function and stepwise single-nucleotide DNA strand translocation through a protein nanopore. *Angew. Chem. Int. Ed. Engl.* 49:10106–10109.
14. Manrao, E. A., I. M. Derrington, …, J. H. Gundlach. 2012. Reading DNA at single-nucleotide resolution with a mutant MspA nanopore and ϕ29 DNA polymerase. *Nat. Biotechnol.* 30:349–353.
15. Lu, B., F. Albertorio, …, J. A. Golovchenko. 2011. Origins and consequences of velocity fluctuations during DNA passage through a nanopore. *Biophys. J.* 101:70–79.
16. Gershow, M., and J. A. Golovchenko. 2007. Recapturing and trapping single molecules with a solid-state nanopore. *Nat. Nanotechnol.* 2:775–779.
17. Mihovilovic, M., N. Hagerty, and D. Stein. 2013. Statistics of DNA capture by a solid-state nanopore. *Phys. Rev. Lett.* 110:028102.
18. Hoogerheide, D. P., B. Lu, and J. A. Golovchenko. 2014. Pressure-voltage trap for DNA near a solid-state nanopore. *ACS Nano.* 8:7384–7391.
19. Rodriguez-Larrea, D., and H. Bayley. 2013. Multistep protein unfolding during nanopore translocation. *Nat. Nanotechnol.* 8:288–295.
20. Hoogerheide, D. P., P. A. Gurnev, …, S. M. Bezrukov. 2017. Mechanism of α-synuclein translocation through a VDAC nanopore revealed by energy landscape modeling of escape time distributions. *Nanoscale.* 9:183–192.
21. Nivala, J., D. B. Marks, and M. Akeson. 2013. Unfoldase-mediated protein translocation through an α-hemolysin nanopore. *Nat. Biotechnol.* 31:247–250.
22. Restrepo-Pérez, L., S. John, …, C. Dekker. 2017. SDS-assisted protein transport through solid-state nanopores. *Nanoscale.* 9:11685–11693.
23. Wilson, J., L. Sloman, …, A. Aksimentiev. 2016. Graphene nanopores for protein sequencing. *Adv. Funct. Mater.* 26:4830–4838.
24. Rostovtseva, T. K., P. A. Gurnev, …, S. M. Bezrukov. 2015. α-Synuclein shows high affinity interaction with voltage-dependent anion channel, suggesting mechanisms of mitochondrial regulation and toxicity in parkinson disease. *J. Biol. Chem.* 290:18467–18477.
25. Hoogerheide, D. P., F. Albertorio, and J. A. Golovchenko. 2013. Escape of DNA from a weakly biased thin nanopore: experimental evidence for a universal diffusive behavior. *Phys. Rev. Lett.* 111:248301.
26. Das, D., and B. A. Krantz. 2016. Peptide- and proton-driven allosteric clamps catalyze anthrax toxin translocation across membranes. *Proc. Natl. Acad. Sci. USA.* 113:9611–9616.
27. Basilio, D., P. K. Kienker, …, A. Finkelstein. 2011. A kinetic analysis of protein transport through the anthrax toxin channel. *J. Gen. Physiol.* 137:521–531.
28. Simon, S. M., C. S. Peskin, and G. F. Oster. 1992. What drives the translocation of proteins? *Proc. Natl. Acad. Sci. USA.* 89:3770–3774.